

# Adsorption and Structural Properties of Ordered Mesoporous Carbons Synthesized by Using Various Carbon Precursors and Ordered Siliceous $P6mm$ and $Ia\bar{3}d$ Mesostructures as Templates

Kamil P. Gierszal,<sup>†</sup> Tae-Wan Kim,<sup>‡</sup> Ryong Ryoo,<sup>\*,‡</sup> and Mietek Jaroniec<sup>\*,†</sup>

Department of Chemistry, Kent State University, Kent, Ohio 44242, USA National Creative Research Initiative Center for Functional Nanomaterials and Department of Chemistry (School of Molecular Science BK21), KAIST, Daejeon 305-701, Republic of Korea

Received: August 14, 2005; In Final Form: October 13, 2005

Adsorption and structural properties of inverse carbon replicas of two ordered siliceous  $P6mm$  and  $Ia\bar{3}d$  mesostructures have been studied by nitrogen adsorption, powder X-ray diffraction, and transmission electron microscopy. These carbon replicas were prepared by filling the pores of SBA-15 and KIT-6 siliceous templates with various carbon precursors followed by carbonization and silica dissolution. Sucrose, furfuryl alcohol, acenaphthene, mesophase pitch, and petroleum pitch were used to obtain inverse carbon replicas of SBA-15 and KIT-6. While structural properties of the resulting ordered mesoporous carbons are mainly determined by the hard template used, their adsorption properties depend on the type of the carbon precursor.

## Introduction

Ordered mesoporous carbons (OMCs) constitute a class of nanomaterials being intensively developed in recent years. Numerous recipes have been proposed to create novel OMCs of complex structures by using various carbon precursors and optimizing synthesis conditions (see review articles<sup>1–5</sup> and references therein). Almost all OMCs have been prepared by employing hard templates. Usually, ordered mesoporous silicas (OMSs) of different structures such as MCM-48, SBA-15, and SBA-16 were used as templates to prepare carbon replicas called CMK-1,<sup>6</sup> CMK-3,<sup>7</sup> and CMK-6,<sup>8</sup> respectively. Numerous studies were done on the carbon replicas of OMSs using carbon precursors with considerable percentage of oxygen and other elements that are usually released in the gaseous form during carbonization process. Recently, another kind of carbon precursor was employed for the synthesis of OMCs, which featured much higher carbon content. Namely, the synthetic mesophase pitch was used in 2001 by Li and Jaroniec<sup>9</sup> to prepare so-called colloid-imprinted mesoporous carbons, and two years later the natural petroleum pitch was applied to obtain the OMS-templated carbons.<sup>10</sup> The mesophase pitch, in contrast to the petroleum pitch, is a mixture of naphthalene-derived compounds exhibiting liquid-crystal arrangement of discotic polyaromatic molecules. In the confinement of silica templates the disk-like molecules of this precursor favor often the edge-on surface anchoring and exhibit perpendicular orientation to the silica pore walls.<sup>11,12</sup> Therefore, TEM images of the mesophase pitch-based OMCs usually show the parallel ordering of graphene sheets that are orthogonal to the surface of template.<sup>13</sup> The use of this kind of pitch is advantageous over the petroleum one because it yields carbons with negligible amount of micropores (pores of widths below 2 nm) due to a small percentage (below 20%) of non-carbon elements in the mesophase pitch, which are micropore-creating agents.

The aforementioned work of Li and Jaroniec<sup>9</sup> reports the synthesis of mesoporous carbons with uniform spherical mesopores generated by imprinting silica colloids in mesophase pitch particles. The amount of created mesopores in pitch particles can be controlled by air stabilization of the pitch–silica nanocomposite that precedes the carbonization process.<sup>14</sup> These studies later by Jaroniec et al.<sup>15–17</sup> resulted in the successful graphitization of colloid-imprinted carbons<sup>15</sup> and in the synthesis of pitch-based carbons with pores created by SBA-15 particles<sup>16</sup> as well as with pores created by both SBA-15 and silica colloids.<sup>17</sup> Independently, a French group reported the synthesis of petroleum pitch-based OMCs by using MCM-48 and SBA-15 as hard templates.<sup>10</sup> The aforementioned studies stimulated interest in the use of pitch and related carbon precursors for the synthesis of OMCs. Kim et al.<sup>13</sup> reported a recipe to obtain the OMCs with partially graphitic pore walls via in-situ conversion of aromatic acenaphthene to mesophase pitch catalyzed by Al-sites of the aluminum-containing MCM-48, SBA-1, and SBA-15. Li et al.<sup>18</sup> reported an interesting method for fluorination of the pitch-based OMCs prepared by using MCM-48 as template. Recently, Yang et al.<sup>19</sup> demonstrated a new approach for the synthesis of carbon nanofiber bundles formed by using pitch with low softening temperature and OMS templates. This work shows that the doping of Fe<sub>2</sub>O<sub>3</sub> catalyst nanoparticles into OMSs allows one to obtain spiral graphitic structures of partially ordered bundles at a quite low temperature (~900 °C) in comparison to that when no catalyst was used. However, when the synthesis was carried out without catalyst, a rigid carbon replica of the OMS template was obtained.

This work is focused on the adsorption and structural properties of OMCs synthesized from various carbon precursors used to fill two OMS templates, SBA-15 with  $P6mm$  symmetry (2D hexagonal structure)<sup>20</sup> and KIT-6 (3D cubic structure).<sup>21–23</sup> KIT-6 exhibits cubic  $Ia\bar{3}d$  symmetry and its structure consists of the interpenetrating bicontinuous network of channels such as those in MCM-48. In contrast to MCM-48, these two intertwined systems of relatively large channels in KIT-6 can

\* Corresponding authors. (Ryoo) E-mail: rryoo@kaist.ac.kr; (Jaroniec) Phone: 330-672-3790; Fax: 330-672-3816; E-mail: jaroniec@kent.edu.

<sup>†</sup> Kent State University.

<sup>‡</sup> Korea Advanced Institute of Science and Technology.

also be connected through irregular micropores present in the mesopore walls analogous to those in SBA-15.<sup>24</sup> Because of this feature it was possible to obtain a faithful carbon replica (CMK-3) of SBA-15, which exhibits a 2D hexagonal arrangement of mesorods.<sup>7</sup> Therefore, in this study, two different mesostructures, SBA-15 and KIT-6, were used to prepare carbon replicas from various precursors (such as sucrose, furfuryl alcohol, acenaphthene, mesophase pitch, and petroleum pitch) in order to investigate a series of OMCs of different adsorption and structural properties by using nitrogen adsorption, powder X-ray diffraction (XRD), and transmission electron microscopy (TEM). A special emphasis is put on OMCs with partially graphitic structures, i.e., those synthesized from pitch or related carbon precursors.

## Experimental Section

**Silica Templates.** *SBA-15.* SBA-15 mesoporous silica (2D hexagonal  $P6mm$  symmetry) was synthesized using the recipe reported by Choi et al.,<sup>25</sup> except the application of hydrothermal treatment at 150 °C for 24 h with the silica/surfactant molar ratio equal to 100. In a typical synthesis batch, 69.1 g of the Pluronic P123 block copolymer (EO<sub>20</sub>PO<sub>70</sub>EO<sub>20</sub>, EO = ethylene oxide, PO = propylene oxide, MW = 5800, Aldrich) was dissolved in 432 g of distilled water and 90 g of 35 wt % HCl solution at 35 °C. 857 g of 5% sodium silicate (DC Chemical, 25 wt % SiO<sub>2</sub> in aqueous solution, Si/Na = 1.5) was added into the aforementioned acidic solution of P123 polymer under stirring at 35 °C, which was continued for 24 h at the same temperature. The mixture was placed in an autoclave and heated at 150 °C for 24 h. The final product was filtered without washing and dried in an oven at 100 °C. The removal of polymeric template was initiated via extraction with an ethanol–HCl mixture and completed via calcination at 550 °C. The calcined SBA-15 silica was then converted to the aluminosilicate form with Si/Al ratio of 20 by the postsynthesis treatment reported previously.<sup>26,27</sup> The Al-incorporated sample is denoted as Al-SBA-15.

*KIT-6.* Large-pore mesoporous silica KIT-6 (cubic  $Ia\bar{3}d$  symmetry) was synthesized according to the procedure described elsewhere.<sup>21,22</sup> Typically, 32 g of P123 and *n*-butanol (Aldrich, 99.4%) were dissolved in 1160 g of distilled water and 63 g of 35 wt % HCl solution under stirring at 35 °C. Tetraethyl orthosilicate (TEOS, 98%, Acros) was added into the aforementioned solution at 35 °C and the magnetic stirring was continued for 24 h at the same temperature. Subsequently, the mixture was placed in an oven at 100 °C for 24 h. The remainder of the synthesis recipe is the same as for SBA-15. The Al-incorporated KIT-6 is denoted as Al-KIT-6.

### Synthesis of OMCs from Various Carbon Precursors.

*Sucrose.* Synthesis of OMCs from sucrose was performed according to a slightly modified recipe reported previously.<sup>6,7</sup> The amounts of sucrose and sulfuric acid were adjusted in relation to the mesopore volume of silica template. Carbonization was performed under atmospheric pressure instead of vacuum. Briefly, calcined silica was infiltrated twice with sucrose solution containing sulfuric acid catalyst. The carbon/silica composite was obtained after complete carbonization at 900 °C under atmospheric pressure using a quartz reactor equipped with porous plug. The mesoporous carbon product was collected on a filter after silica template dissolution with HF solution. The mesoporous carbon replicas of the SBA-15 and KIT-6 silica templates are designated as CMK3-SC and CMK8-SC, respectively.

*Furfuryl Alcohol.* Synthesis of OMCs from furfuryl alcohol precursor was essentially the same as that reported in our

previous work<sup>8</sup> involving Al-SBA-16 template for the preparation of a cubic  $Im\bar{3}m$  OMC. A slight modification of this procedure involved the adjustment of the amount of furfuryl alcohol in relation to the pore volume of silica template. Briefly, this recipe was as follows: furfuryl alcohol was infiltrated into aluminosilicate at room temperature and polymerized at 95 °C. The resultant polymer/aluminosilicate composite sample was further heated at 350 °C. After cooling the sample to room temperature, additional furfuryl alcohol was added. This sample was heated at 95 °C and again at 350 °C. Carbonization was completed at 900 °C under self-generated gas atmosphere using a quartz reactor equipped with porous plug. The Al-SBA-15 and Al-KIT-6 silica templates were removed with HF solution. The resulting OMCs are denoted as CMK3-FA and CMK8-FA, respectively.

*Acenaphthene.* Synthesis of OMCs from acenaphthene was performed as described previously,<sup>13</sup> except for the difference in the amount of carbon precursor adjusted to the mesopore volume of silica template. Briefly, this recipe was as follows: a physical mixture of acenaphthene and aluminosilicate was placed in an autoclave and heated at 750 °C in a muffle furnace. After being cooled to room temperature, the product was moved into a fused quartz reactor, which was equipped with fritted disks. Carbonization was performed by heating the reactor at 900 °C under vacuum conditions. The carbons prepared by using Al-SBA-15 and Al-KIT-6 as templates are denoted as CMK3-AN and CMK8-AN, respectively.

*AR Mesophase Pitch.* Synthesis of OMCs from AR mesophase pitches was carried out as follows: 1.56 g of ground naphthalene-based (NP) or methyl naphthalene-based (MNP) AR mesophase pitches (donated by Mitsubishi Gas Chemical Co., Japan) with softening point (SP) temperatures 209, 273, 283.7, and 251 °C for NP209, NP273, NP283, and MNP251, respectively, and 1 g of SBA-15 (or 1.25 g of AR pitch per 1 g of KIT-6) were put together in polypropylene bottle with 10 mL of ethanol. After agitation of this mixture for 30 min, ethanol was evaporated at 100 °C in an oven. The dried mixture was moved to a quartz reactor equipped with porous plug and heated in a furnace with a temperature increase at a rate of 1.4 °C min<sup>-1</sup> to exceed SP of each pitch by 30 °C. After maintaining the aforementioned infiltration temperature of the mixture for 4 h, it was heated to 900 °C with a rate of 2.6 °C min<sup>-1</sup> and remained at this temperature for 2 h. The product was collected after cooling the quartz reactor to room temperature. The resulting OMCs were recovered by removal of the SBA-15 and KIT-6 silica templates with HF solution. The samples are denoted as CMK3-X and CMK8-X, respectively, where X = NP209, NP273, NP283, and MNP251.

*Petroleum Pitch.* Two different procedures were used to synthesize mesoporous carbons from Ashland A240 petroleum pitch (donated from Mitsubishi Gas Chemical Co., Japan). The first procedure is the same as that described above for the synthesis of OMCs from the AR mesophase pitches, except for the difference in the infiltration temperature (302 °C for A240 pitch) during carbonization. The carbon samples obtained by using the SBA-15 and KIT-6 OMS templates are denoted as CMK3-A240 and CMK8-A240, respectively.

The second procedure for the synthesis of OMCs from Ashland A240 petroleum pitch was performed according to the recipe reported by the French group.<sup>10</sup> Briefly, the silica templates were impregnated with pitch at 302 °C under stirring for 4 h and cooled to 102 °C. Next, carbonization was done at 950 °C under flowing argon. The resultant carbon samples

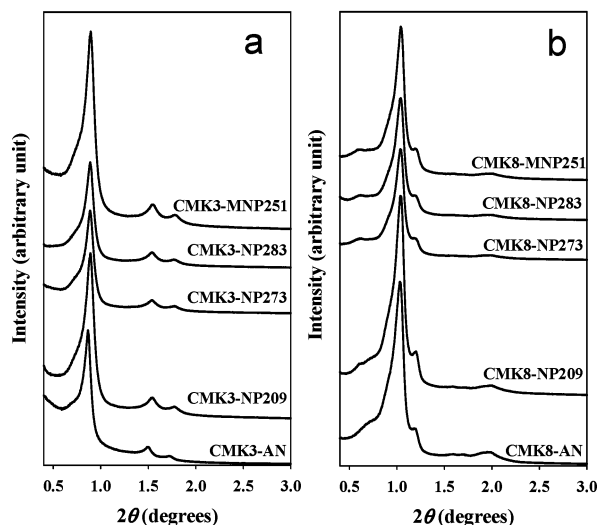


**Figure 1.** Low-angle XRD patterns for the CMK3 (a) and CMK8 (b) OMCs prepared from various AR mesophase pitches and acenaphthene.

obtained by using SBA-15 and KIT-6 as templates are denoted CMK3-A240\* and CMK8-A240\*, respectively.

**Measurements.** Synchrotron powder X-ray diffraction (XRD) patterns at low angles were collected using BL8C2 beam line at Pohang Light Source in the reflection mode ( $\lambda = 0.15444$  nm). The XRD patterns at high angles were recorded on a Rigaku Multiplex instrument using Cu K $\alpha$  radiation ( $\lambda = 0.15406$  nm) operated at 50 kV and 30 mA (1.5 kW) in step scan mode.

Transmission electron microscopy (TEM) images were taken from thin edges of particles supported on a porous carbon grid using JEOL JEM-3010 equipment operated at 300 kV.

Nitrogen adsorption isotherms were measured at  $-196$  °C on a Micromeritics ASAP 2010 volumetric adsorption analyzer. Before the adsorption measurements all samples were outgassed at  $200$  °C in the degas port of the adsorption analyzer.

## Results and Discussion

### XRD and TEM Studies of Structural Properties of OMCs.

As shown in Figure 1, each XRD pattern for the OMCs prepared from AR mesophase pitches and acenaphthene showed more than three distinct reflections in the range of  $2\theta$  below  $3.0^\circ$ , which are characteristic for highly ordered mesostructures belonging to 2D hexagonal  $P6mm$  and 3D cubic  $Ia\bar{3}d$  space groups, respectively. The XRD patterns for OMCs shown in this figure match exactly the patterns for the corresponding SBA-15 and KIT-6 silica templates (see Supporting Information Figure S1), which indicates that the aforementioned OMCs are faithful inverse replicas of those templates.

The unit cell parameters for the SBA-15 and KIT-6 templates and the corresponding OMC samples evaluated from the XRD data are summarized in Tables 1 and 2. As can be seen from these tables, a slight contraction of the unit cell is observed in the case of the OMCs prepared from acenaphthene, AR mesophase pitches, and A240 petroleum pitch. The degree of contraction for the pitch-based OMCs synthesized by single step infiltration is similar to that for the OMC prepared from furfuryl alcohol by double infiltration, but this contraction is much lower than that for the sucrose-based OMCs (see Supporting Information Figures S2 and S3). This lower shrinkage of the pitch-based OMCs in comparison to the sucrose-based OMCs is related to much higher coke yield in the case of pitch carbonization.<sup>9</sup>

**TABLE 1: Adsorption and Structural Parameters for the CMK3 Series of OMCs**

| Sample      | $a$ [nm] | $S_{\text{BET}}$ [m <sup>2</sup> /g] | $S_{\text{ex}}$ [m <sup>2</sup> /g] | $V_t$ [cc/g] | $w_{\text{KJS}}$ [nm] |
|-------------|----------|--------------------------------------|-------------------------------------|--------------|-----------------------|
| SBA-15      | 12.17    | 510                                  | 100                                 | 1.2          | 10.85                 |
| CMK3-SC     | 10.32    | 660                                  | 10                                  | 1.0          | 5.75                  |
| CMK3-FA     | 11.17    | 920                                  | 60                                  | 1.08         | 6.25                  |
| CMK3-AN     | 11.81    | 240                                  | 220                                 | 0.43         | 5.56                  |
| CMK3-NP209  | 11.48    | 320                                  | 100                                 | 0.42         | 4.54                  |
| CMK3-NP273  | 11.49    | 210                                  | 40                                  | 0.26         | 4.7                   |
| CMK3-NP283  | 11.49    | 210                                  | 50                                  | 0.27         | 4.66                  |
| CMK3-MNP251 | 11.42    | 260                                  | 60                                  | 0.35         | 4.8                   |
| CMK3-A240*  | 11.17    | 740                                  | 140                                 | 0.69         | 5.0                   |
| CMK3-A240   | 11.44    | 420                                  | 100                                 | 0.52         | 4.66                  |

$a$  = unit cell parameter,  $S_{\text{BET}}$  = BET surface area,  $S_{\text{ex}}$  = external surface area,  $V_t$  = single-point pore volume, and  $w_{\text{KJS}}$  = pore width at the maximum of PSD evaluated by the KJS method.

**TABLE 2: Adsorption and Structural Parameters for the CMK8 Series of OMCs**

| Sample      | $a$ [nm] | $S_{\text{BET}}$ [m <sup>2</sup> /g] | $S_{\text{ex}}$ [m <sup>2</sup> /g] | $V_t$ [cc/g] | $w_{\text{KJS}}$ [nm] |
|-------------|----------|--------------------------------------|-------------------------------------|--------------|-----------------------|
| KIT-6       | 23.07    | 740                                  | 20                                  | 0.95         | 8.86                  |
| CMK8-SC     | 19.44    | 670                                  | 20                                  | 0.89         | 5.34                  |
| CMK8-FA     | 21.15    | 960                                  | 70                                  | 0.99         | 4.90                  |
| CMK8-AN     | 20.96    | 370                                  | 60                                  | 0.42         | 4.70                  |
| CMK8-NP209  | 20.85    | 500                                  | 60                                  | 0.49         | 4.17                  |
| CMK8-NP273  | 20.86    | 290                                  | 70                                  | 0.29         | 4.17                  |
| CMK8-NP283  | 20.84    | 320                                  | 80                                  | 0.32         | 4.16                  |
| CMK8-MNP251 | 20.75    | 370                                  | 90                                  | 0.39         | 4.30                  |
| CMK8-A240*  | 21.68    | 1250                                 | 20                                  | 1.10         | 4.57                  |
| CMK8-A240   | 21.36    | 660                                  | 100                                 | 0.61         | 4.07                  |

$a$  = unit cell parameter,  $S_{\text{BET}}$  = BET surface area,  $S_{\text{ex}}$  = external surface area,  $V_t$  = single-point pore volume, and  $w_{\text{KJS}}$  = pore width at the maximum of PSD evaluated by the KJS method.

The wide-angle XRD patterns for the OMCs synthesized from various carbon precursors are shown in the Supporting Information Figure S4. The OMC samples prepared from AR mesophase pitch NP209 and acenaphthene show distinct peaks around  $2\theta = 26^\circ$  and  $45^\circ$ , which correspond to the (002) and (101) reflections characteristic for graphitic domains. However, the wide-angle XRD pattern for CMK3-A240\* prepared from A240 petroleum pitch shows broad and weak reflections in comparison to those observed for the CMK3-A240 sample, which was obtained from the same carbon precursor. The broad XRD peaks for CMK3-A240\* indicate that the degree of graphitization in this carbon sample is small, which might be caused by oxidative stabilization of the pitch-OMS composite in air done before its carbonization. The removal of oxygen-containing groups during carbonization, which were created during air stabilization, may reduce the size of graphitic domains in the aforementioned carbon sample.

Shown in Figure 2 are the representative TEM images for the CMK3-NP209 and CMK8-NP209 OMCs. These images show clearly that the AR pitch-based carbon replicas exhibit a long range ordering with 2D hexagonal  $P6mm$  and 3D cubic  $Ia\bar{3}d$  symmetry, respectively. In addition, the high-resolution TEM (HRTEM) image for CMK3-NP209 indicates perpendicular orientation of graphene sheets to the axis of cylindrical channels in the 2D hexagonal structure of SBA-15, which is the same as that reported for the CMK3-AN carbon prepared from acenaphthene.<sup>13</sup>

**Adsorption Properties of Silica Templates.** Nitrogen adsorption isotherms for the SBA-15 and KIT-6 silica templates are shown in Figure 3. A visual analysis of these isotherms shows that the silicas studied are high quality OMSs because they exhibit extremely steep capillary condensation/evaporation

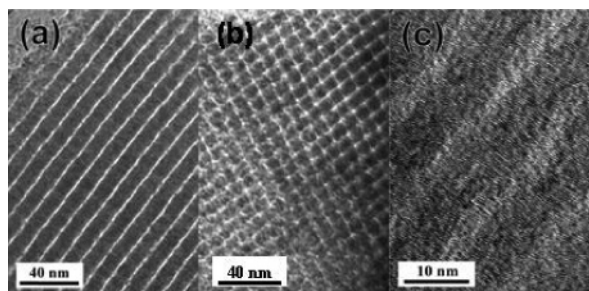


**Figure 2.** TEM images for the CMK3-NP209 (a) and CMK8-NP209 (b) carbons and HRTEM image for CMK3-NP209 (c).

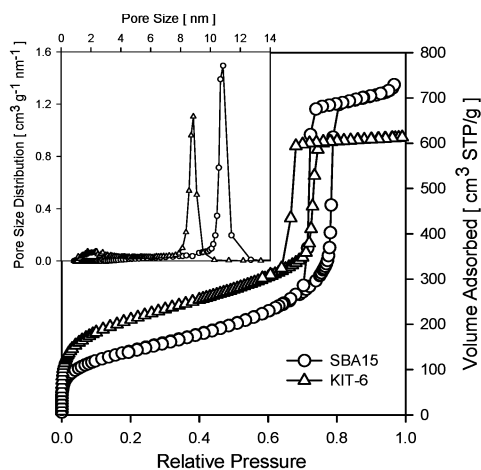


**Figure 3.** Nitrogen adsorption isotherms and corresponding pore size distributions for the SBA-15 and KIT-6 silicas.

steps followed by rather small increase in the amount adsorbed. The former feature reflects a high uniformity of mesopore sizes, while the latter indicates a small textural (secondary) mesoporosity, and consequently a small external surface area,  $S_{\text{ex}}$ . Particularly, the KIT-6 silica studied here fulfilled the latter property because its external surface area is about 20 m<sup>2</sup>/g. A high quality of the OMS template is of paramount significance for the preparation of high quality inverse replicas because they inherit easily all imperfections of the templates used. Each replication usually broadens the resulting PSD.

The SBA-15 and KIT-6 silica templates studied here possessed the BET specific surface areas of 510 m<sup>2</sup>/g and 740 m<sup>2</sup>/g, and the total pore volumes of 1.2 cm<sup>3</sup>/g and 0.95 cm<sup>3</sup>/g, respectively. The high total pore volume and the volume of primary mesopores for SBA-15 are due to the 24 h hydrothermal treatment done at relatively high temperature, 150 °C. This treatment had a positive effect on the pore volume but caused reduction of the pore wall thickness. The superior uniformity of pore sizes in the silicas studied is reflected by very narrow pore size distributions (PSDs), shown in the inset of Figure 3. The mesopore widths at the maximum of those PSDs are equal to 10.85 and 8.86 nm for SBA-15 and KIT-6, respectively, indicating the presence of large and uniform mesopores in these materials.

**Adsorption Properties of Inverse Carbon Replicas of SBA-15.** Adsorption properties of carbon replicas of SBA-15 depend on the type of the carbon precursor used (see Figure 4). The OMCs prepared from mesophase pitch with high SP, CMK3-NP273, and CMK3-NP283, revealed the low total pore volume and the small BET specific surface area. This can be attributed to the fact that the carbonized high SP pitch contains a considerable amount of large polyaromatic compounds, which, after carbonization, afford OMC with extremely low mi-

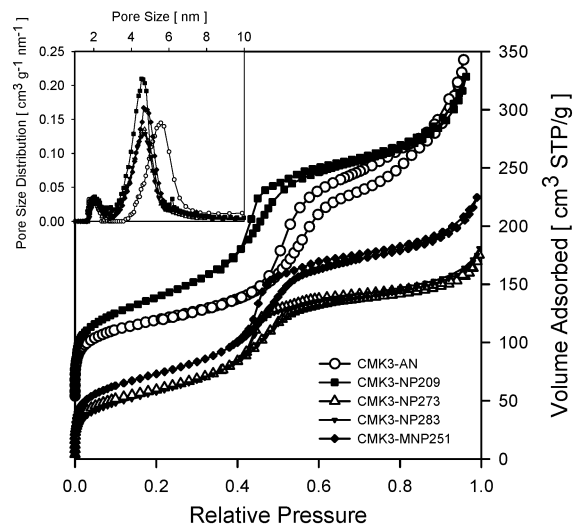


**Figure 4.** Nitrogen adsorption isotherms and corresponding pore size distributions for the carbon replicas synthesized from acenaphthene (AN), methyl naphthalene-based mesophase pitch (MNP) and naphthalene-based mesophase pitches (NP) with different softening point and the SBA-15 template. The adsorption isotherms for the CMK3-AN and CMK3-NP209 have been shifted vertically by 50 cm<sup>3</sup>/g.

croporosity. Since the aforementioned carbons were made from pitches of similar properties, their nitrogen adsorption isotherms are close to each other. The carbons obtained from pitches with lower SP possessed not only higher total pore volumes but also greater secondary porosity, which indicates some deterioration of their ordered structures. This is manifested by a steady increase of the adsorption isotherm curve, which appears after the step reflecting capillary condensation in primary mesopores. Such shape of the nitrogen adsorption isotherm was also obtained for CMK3-AN, which in this case may be caused by specific synthesis conditions involving in-situ creation of mesophase pitch inside channels of the SBA-15 template. On the other hand, the OMCs synthesized from the carbon precursors giving much lower coke yield such as sucrose, furfuryl alcohol, and petroleum pitch (see Supporting Information Figures S5 and S6) exhibited also relatively low external surface areas and large total pore volume. This means that these OMCs possessed a small amount of secondary mesopores and simultaneously a large amount of irregular micropores located in the mesopore walls. Furthermore, the use of this kind of precursors caused a significant shrinkage of the whole carbon structure, which is especially visible in the case of OMCs prepared from sucrose. For instance, the drop in the  $d$ -spacing value for CMK3-SC after carbonization was  $\sim 15\%$ . Note that the third power of the ratio of the  $d$  spacing values for the sample after and before carbonization gives an approximate percentage of the coke yield, providing that the shrinkage was the same in all three dimensions. In the case of the carbon made from sucrose, this quantity was  $\sim 61\%$ , whereas in the case of the carbon from the low SP mesophase pitch it reached 84%. One can infer from the geometrical calculations that the distance between carbon nanorods in the SBA-15 replica should be equal to or greater than the wall thickness of the template. This conclusion is confirmed by the TEM image of CMK3-NP209 presented in Figure 2.

In general, the isotherm curves for the OMCs studied reveal narrow loops closing at the lower limit adsorption–desorption hysteresis that, for nitrogen at  $-196$  °C, occurs at a relative pressure of about 0.4 (see Figure 4). The pore size distributions (inset in Figure 4) obtained from nitrogen adsorption isotherms

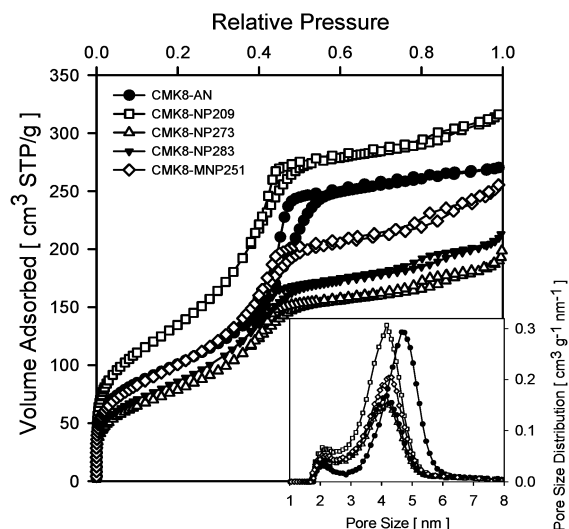


**Figure 5.** Nitrogen adsorption isotherms and the corresponding pore size distributions for the carbon replicas synthesized from acenaphthene (AN), methyl naphthalene-based mesophase pitch (MNP), and naphthalene-based mesophase pitches (NP) with different softening points and the KIT-6 template.

for the mesophase pitch-based carbons reveal narrow peaks attributed to the primary mesopores and very small ones located around 2 nm reflecting microporosity. A similar location of almost all main peaks of PSDs indicates that the average width of primary mesopores was analogous for all OMCs studied, and its value was about 4.7 nm (Table 1). An exception is the result obtained for CMK3-AN, for which the mesopore width was 5.56 nm. The mesopore diameters for the carbons synthesized from other precursors attained relatively high values due to the significant shrinkage of their structures during carbonization process. Note that a more quantitative comparison of the pore diameters of the OMS templates and their inverse carbon replicas is difficult because the pore geometries in these materials are different. For instance, in the case of SBA-15 its mesopores have cylindrical shape, whereas in the case of its inverse carbon replica their shape is determined by the space between hexagonally ordered carbon nanorods. Since for both types of materials the pore size analysis was done by assuming cylindrical geometry (the KJS method based on the BJH algorithm),<sup>28</sup> it led to some overestimation of the mesopore widths in the case of CMK-3 as indicated elsewhere.<sup>8</sup>

**Adsorption Properties of Carbon Inverse Replicas of KIT-6.** As mentioned above, the MCM-48-like 3D structure of the KIT-6 silica prepared by employing an analogous polymeric template as that used in the synthesis of SBA-15 is a superior mold for carbon replication. The nitrogen adsorption isotherms for the carbon replicas of KIT-6 (Figure 5) indicate a high quality of these materials, which had relatively low external surface areas. This result could be expected because carbon replicas inherited the aforementioned feature from the KIT-6 template, which showed a very small amount of textural (secondary) mesopores. The total nitrogen adsorption capacity of the carbons made from the mesophase pitches was the highest for CMK8-NP209 and the lowest for CMK8-273 and CMK8-283. This behavior is similar to that observed for the corresponding carbon replicas of SBA-15 and it confirms again a significant influence of the mesophase pitch softening point on the properties of the resulting carbon replicas. It seems clear that the lower SP of mesophase pitch the higher amount of fine pores is formed. The BET specific surface areas of the KIT-6-templated carbons ranged from 290 m<sup>2</sup>/g to 500 m<sup>2</sup>/g and

their total pore volumes varied from 0.29 cm<sup>3</sup>/g to 0.49 cm<sup>3</sup>/g (Table 2). The OMCs synthesized from sucrose and furfuryl alcohol featured much higher nitrogen adsorption (see Supporting Information Figures S5 and S6). In the case of the KIT-6-templated carbons one could also expect a decrease in the *d*-spacing indicating some structure shrinkage, the degree of which was expectedly the highest for the sucrose-based OMCs.

For pitch-based carbon replicas of KIT-6 the capillary condensation step occurs at a relative pressure of about 0.4. Therefore, nitrogen adsorption isotherms at −196 °C for these carbons show very narrow hysteresis loops because the lower limit of their closure is also about 0.4. A visual analysis of the pore size distributions for these carbons (inset in Figure 5) shows that the positions of their maxima are very similar, i.e., about 4.2 nm except CMK8-AN, for which the pore width is about 4.7 nm. For OMCs prepared from sucrose and furfuryl alcohol, this mesopore width is even higher. The PSD peaks for all KIT-6-templated OMCs are quite narrow except those for CMK8-SC and CMK8-A240. Here again one needs to take into account an overestimation of the pore widths estimated by the BJH–KJS method, which is applicable for cylindrical mesopores.<sup>28</sup>

## Conclusions

This study shows that the KIT-6 silica exhibiting 3D bicontinuous network of large channels with interconnecting micropores in the mesopore walls constitutes an excellent template for the preparation of its faithful inverse replica. Taking advantage of this structure, its carbon replicas were obtained from various carbon precursors such as sucrose, furfuryl alcohol, and mesophase pitches with different softening points, and their adsorption properties were studied. It was shown that the softening point of mesophase pitch has a pronounced influence on the properties of the resulting OMCs. One of the most significant features of the pitch-based OMCs is the possibility of controlling their microporosity and consequently the ability to prepare OMCs without irregular micropores. For instance, OMC obtained from a naphthalene-derived mesophase pitch with high softening point exhibited an unusually small amount of micropores. In addition, the pitch-based carbons with sufficiently thick pore walls are relatively easily graphitized.<sup>19,29</sup>

**Acknowledgment.** This work was supported in part by the donors of Creative Research Initiative Program of the Korean Ministry of Science and Technology (R.R.), School of Molecular Science through the Brain Korea 21 project (R.R.), and NSF Grant CHE-0093707 (M.J.). Synchrotron radiation XRD experiments at PLS were supported in part by MOST and POSTECH. The authors also thank Mitsubishi Gas Chemical Co. for the donation of AR mesophase pitches.

**Supporting Information Available:** Supporting figures S1–S6. This material is available free of charge via the Internet at <http://pubs.acs.org>.

## References and Notes

- (1) Ryoo, R.; Joo, S. H.; Kruk, M.; Jaroniec, M. *Adv. Mater.* **2001**, *13*, 667.
- (2) Lee, J.; Han, S.; Hyeon, T. *J. Mater. Chem.* **2004**, *14*, 478.
- (3) Lebeau, B.; Parmentier, J.; Souillard, M.; Fowler, C.; Zana, R.; Vix-Guter, C.; Patarin, J. *Comptes Rendus Chim.* **2005**, *8*, 597.
- (4) Yang, H. F.; Zhao, D. Y. *J. Mater. Chem.* **2005**, *15*, 1217.
- (5) Sakintuna, B.; Yurum, Y. *Ind. Eng. Chem. Res.* **2005**, *44*, 2893.
- (6) Ryoo, R.; Joo, S. H.; Jun, S. *J. Phys. Chem. B* **1999**, *103*, 7743.
- (7) Jun, S.; Joo, S. H.; Ryoo, R.; Kruk, M.; Jaroniec, M.; Liu, Z.; Ohsuna, T.; Terasaki, O. *J. Am. Chem. Soc.* **2000**, *122*, 10712.

- (8) Kim, T.-W.; Ryoo, R.; Gierszal, K. P.; Jaroniec, M.; Solovyov, L. A.; Sakamoto, Y.; Terasaki, O. *J. Mater. Chem.* **2005**, *15*, 1560.
- (9) Li, Z.; Jaroniec, M. *J. Am. Chem. Soc.* **2001**, *123*, 9208.
- (10) Vix-Guterl, C.; Saadallah, S.; Vidal, L.; Reda, M.; Parmentier, J.; Patarin, J. *J. Mater. Chem.* **2003**, *13*, 2535.
- (11) Yang, N. Y. C.; Jian, K.; Kulaots, I.; Crawford, G. P.; Hurt, R. H. *J. Nanosci. Nanotechnol.* **2003**, *3*, 386.
- (12) Hurt, R.; Krammer, G.; Crawford, G. P.; Jian, K.; Rulison, C. *Chem. Mater.* **2002**, *14*, 4558.
- (13) Kim, T.-W.; Park, I.-S.; Ryoo, R. *Angew. Chem., Int. Ed.* **2003**, *42*, 4375.
- (14) Li, Z.; Jaroniec, M. *Chem. Mater.* **2003**, *15*, 1327.
- (15) Li, Z.; Jaroniec, M.; Lee, Y. J.; Radovic, L. R. *Chem. Commun.* **2002**, 1346.
- (16) Li, Z.; Jaroniec, M. *J. Phys. Chem. B* **2004**, *108*, 824.
- (17) Gierszal, K. P.; Jaroniec, M. *Chem. Commun.* **2004**, 2576.
- (18) Li, Z.; del Cul, G. D.; Yan, W.; Liang, C.; Dai, S. *J. Am. Chem. Soc.* **2004**, *108*, 12782.
- (19) Yang, H.; Yan, Y.; Liu, Y.; Zhang, F.; Zhang, R.; Meng, Y.; Li, M.; Xie, S.; Tu, B.; Zhao, D. *J. Phys. Chem. B* **2004**, *108*, 17320.
- (20) Zhao, D. Y.; Feng, J. L.; Huo, Q. S.; Melosh, N.; Fredrickson, G. H.; Chmelka, B. F.; Stucky, G. D. *Science* **1998**, *279*, 548.
- (21) Kleitz, F.; Choi, S. H.; Ryoo, R. *Chem. Comm.* **2003**, 2136.
- (22) Kim, T.-W.; Kleitz, F.; Paul B., Ryoo, R. *J. Am. Chem. Soc.* **2005**, *127*, 7601.
- (23) Sakamoto, Y.; Kim, T.-W.; Ryoo, R.; Terasaki, O. *Angew. Chem., Int. Ed.* **2004**, *43*, 5231.
- (24) Ryoo, R.; Ko, C. H.; Kruk, M.; Antochshuk, V.; Jaroniec, M. *J. Phys. Chem. B* **2000**, *104*, 11465.
- (25) Choi, M.; Heo, W.; Kleitz, F.; Ryoo, R. *Chem. Commun.* **2003**, 1340.
- (26) Ryoo, R.; Jun, S.; Kim, J. M.; Kim, M. J. *Chem. Commun.* **1997**, 2225.
- (27) Jun, S.; Ryoo, R. *J. Catal.* **2000**, *195*, 237.
- (28) Kruk, M.; Jaroniec, M.; Sayari, A. *Langmuir* **1997**, *13*, 6267.
- (29) Yoon, S. B.; Chai, G. S.; Kang, S. K.; Yu, J. S.; Gierszal, K. P.; Jaroniec, M. *J. Am. Chem. Soc.* **2005**, *127*, 4188.